PICOSECOND PULSED LASER ABLATION FOR THE SURFACE PREPARATION OF EPOXY COMPOSITES

Frank Palmieri[1], Rodolfo Ledesma[2], Tayler Fulton[3], Alexandria Arthur[3], Keisharra Eldridge[3], Sheila Thibeault[1], Yi Lin[4], Chris Wohl[1] and John Connell[1]

1. NASA Langley Research Center, Hampton, VA 23681
2. University of Virginia, Charlottesville, VA 22904
3. NASA Internship Program, Hampton, VA 23681
4. National Institute of Aerospace, Hampton, VA 23666

ABSTRACT

As part of a technical challenge under the Advanced Composites Program, methods for improving pre-bond process control for aerospace composite surface treatments and inspections, in conjunction with Federal Aviation Administration guidelines, are under investigation. The overall goal is to demonstrate high fidelity, rapid and reproducible surface treatment and surface characterization methods to reduce uncertainty associated with the bonding process. The desired outcomes are reliable bonded airframe structure, and reduced timeline to certification. In this work, laser ablation was conducted using a q-switched Nd:YVO_4 laser capable of nominal pulse durations of 8 picoseconds (ps). Aerospace structural carbon fiber reinforced composites with an epoxy resin matrix were laser treated, characterized, processed into bonded assemblies and mechanically tested. The characterization of ablated surfaces were conducted using scanning electron microscopy (SEM), water contact angle (WCA) goniometry, micro laser induced breakdown spectroscopy (μLIBS), and electron spin resonance (ESR). The bond performance was assessed using a double cantilever beam (DCB) test with an epoxy adhesive. The surface characteristics and bond performance obtained from picosecond ablated carbon fiber reinforced plastics (CFRPs) are presented herein.

1. INTRODUCTION

Adhesive bonding has several promising advantages over mechanical fastening, particularly in the assembly of composite structures, by reducing manufacturing cost in terms of time, labor and complexity, and enabling new airframe designs with improved performance [1-2]. Currently, Federal Aviation Administration (FAA) certification requirements include redundant load paths (e.g., mechanical fasteners) in secondary-bonded, primary structures (SBPS) because no nondestructive methods exist to directly measure the strength of an adhesive bond. To advance SBPS towards certification per FAA guidance, improvements in process control and tools for rapid analysis of bonding surface quality are needed. A repeatable, effective and measurable surface treatment is a key component of an overall manufacturing methodology for the certification of SBPS[2-4]. In addition, metrology techniques are needed for rapid, in-line assessment of prepared surfaces to assure the surfaces are free of contaminants and activated for bonding in order to achieve repeatable bond performance without destructive testing [5-6].

1.1 State-of-the-Art Surface Preparation

Surface preparation should not be thought of as a stand-alone process. One must consider a "bonding system" which is comprised of the substrate material to be bonded, the surface treatment process conducted on that material, the adhesive, and the process under which bonding is conducted. If any one of these entities is changed, then the outcome, in terms of bond performance, may also change. The purpose of the surface treatment process is to simultaneously remove contaminants and activate the surface for bonding. The term activate implies that chemically reactive species are generated that ideally will chemically react with the adhesive (or bond primer) and create a stable interfacial bond. Once the surface treatment process is performed, the history of the material becomes very important as passivation of the chemically active species and/or contamination of the treated surface can occur, thus the elapsed time and storage environment prior to bonding must be well-controlled. Current surface preparation methods rely on mechanical processes to remove contaminants and create chemically active surfaces. The most common techniques are sanding, grit blasting, and peel-ply. Sanding and grit blasting can be difficult to automate and involve a significant amount of human intervention and judgment that introduces variability. The sanding or grit media can serve as sources of contamination, and their history and re-use has to be well-controlled. Mechanical abrasion is non-selective and can result in fiber damage and leave behind or even embed debris; often a solvent wipe is used in an attempt to remove such debris [7-8]. A peel ply may also leave behind residual debris or a layer of contamination that must be removed before bonding. For acceptable bond performance, the correct peel ply fabric must be paired with a resin matrix and adhesive which further validates the concept of a "bonding system" [9-10].

1.2 Laser Surface Preparation

Laser surface treatment offers a contrast to mechanical abrasion and peel ply techniques in that it is readily controllable, repeatable, and scalable solution to prepare composite surfaces for bonding [11-12]. Laser power, focus, pulse frequency, and translation speed can be controlled with a high degree of fidelity which allow the properties of the treated surface to be highly controlled and reproducible [13]. Ablation is the vaporization and ejection of material from a surface due to the absorption of intense radiation. The wavelength, pulse duration, fluence, and scan parameters of the laser can be set to selectively ablate a desired amount of matrix resin without damaging the carbon fiber. In the report by Fischer et al. [14], it is suggested that maximal epoxy should be removed, while keeping the structure of the load-bearing fibers intact, to enable direct load introduction to the fibers [14-15]. Another consideration with laser surface preparation of composites is that, depending on the amount of matrix resin removed, the failure mode of adhesively bonded specimens can be engineered to occur within the top plies of the bonded laminates versus in the adhesive bond line [15].

Previous work established a process for laser-treated carbon fiber reinforced plastic (CFRP) surfaces using a frequency tripled (355 nm), nanosecond, Nd:YAG laser at varying average laser power and areal coverage [15-17]. Laser parameters were established that gave optimal bond performance based on mode I mechanical tests and were effective in the removal of polydimethylsiloxane contaminates [17]. In this report, the effectiveness of a picosecond pulsed laser system in preparing aerospace structural composites for adhesive bonding, and a novel method (micro laser induced breakdown spectroscopy, μLIBS) to determine the presence of minute quantities of silicone contaminants were investigated.

1.3 Pre-bonding Surface Inspection

The ability to rapidly determine if a treated composite surface is free of contaminants and chemically activated for bonding is a critical aspect of advancing the adhesive bonding process towards FAA certification. The level of certain contaminants, e.g., silicones, that can cause problems in the bonding system studied herein can be as low as 0.8 $\mu g/cm^2$ [17], thus highly sensitive techniques with minimal post interrogation data analysis processes are required. One of the primary sources of contaminants on composites comes from the materials used in the fabrication of said composites, most notably mold release agents used on tools, release plies and release fabrics that come into contact with the prepreg and cured composites. One of the most common ingredients in these mold release products is silicone [polydimethylsiloxane (PDMS) or derivatives thereof]. The rapid detection of silicone contaminants on composites at the low concentrations mentioned is particularly challenging. X-ray photoelectron spectroscopy (XPS) and ion scattering spectroscopy can provide quantitative composition information for the uppermost atomic layers of a surface. Unfortunately, they require a significant amount of sample preparation, data acquisition and analysis time and are not practical for in-line quality assurance processes. Infrared spectroscopy coupled with chemometrics and water contact angle (WCA) techniques are being assessed for the in-line detection of surface contaminant concentrations as low as 1 $\mu g/cm^2$ [6, 17-18]. However, as mentioned previously, PDMS may diminish bond performance at concentrations less than 1 $\mu g/cm^2$. Other techniques that have been investigated include commercial off the shelf hand held x-ray fluorescence and laser induced breakdown spectroscopic instruments, however they currently lack the sensitivity and/or rapid data analysis times needed.

Two techniques currently under investigation by our group include optically stimulated electron emission (OSEE) which was developed primarily for inspection of metallic surfaces for grease residue, and micro-laser induced breakdown spectroscopy (μLIBS) [21]. With regard to work presented herein, the μLIBS approach does not require a separate laser for surface activation as it is combined with the laser surface treatment process. Both methods may be effective for in-line inspection of composite surfaces as they are highly sensitive and give near instantaneous feedback of results with no subsequent data reduction or analysis necessary. μLIBS provides chemical information of the species detected, while OSEE does not. In OSEE, the electric current emitted from a surface exposed to deep ultra violet (DUV) radiation is dependent on the work function of the substrate. Materials with relatively small work functions (i.e., electrical conductors) emit electrons in DUV while dielectrics (i.e., composite matrix resins) are far less likely to emit, thus it is highly sensitive to surface contamination. The inspection is rapid and provides a quantitative assessment of surface contamination levels. However, since the work function of emitted electrons is not measured, the surface chemical composition cannot be directly determined [22]. In μLIBS, radiation from a plasma plume produced during laser ablation is spectroscopically interrogated. The resulting spectrum contains information about surface composition and relative abundance of excited atomic and molecular species in the plasma plume. The time associated with these events is on the picosecond scale, thus the data are obtained in real-time. The energy of each laser pulse used in the surface treatment process is on the micro-joule scale, hence the designation of μLIBS. This means the amount of the material in the generated plasma plume is extremely low, and thus a highly sensitive spectrometer/detector system is required for accurate and reliable detection of contaminant concentrations. Ideally, μLIBS could be integrated with the laser surface preparation process to provide real-time, in-situ monitoring of the surface chemistry and closed-loop control of the ablation process.

1.4 Contents of this Report

A picosecond laser was used to treat CFRPs prior to adhesive bonding. Several laser parameters were investigated, and the effect on the surface chemistry, energy and topography, and mechanical properties of bonded specimens were determined. The ability of the μLIBS system integrated with the picosecond laser to detect low levels of silicone based contaminants was also investigated. The results of this study are presented herein.

2. EXPERIMENTATION

2.1 Materials

Double cantilever beam (DCB) specimens were fabricated from CFRP panels (30.5 cm × 30.5 cm, 12 in × 12 in) that were prepared from 10 plies of Torayca P2302-19 prepreg tape (T800H/3900-2 carbon fiber/toughened epoxy resin system) and cured in an autoclave at 177 °C (350 °F) and 690 kPa (100 psi). Release from the caul plate was accomplished using Airtech A4000 release film [fluorinated ethylene propylene (FEP)]. The panels were laser treated and then adhesively bonded within 48 h. The adhesive used for bonding was Hysol EA9696 from Henkel Corporation. The bonded assemblies were cured in an autoclave at 121 °C (250 °F) and 0.34-0.68 MPa (50-100 psi). The panels were subsequently cut into individual DCB specimens using a water jet. For μLIBS experiments, 8-ply CFRP panels (30.5 cm × 30.5 cm, 12 in × 12 in) were prepared in the same fashion and cut into 3.8 cm × 3.8 cm (1.5 in × 1.5 in) coupons that were used for characterization and test. Samples were contaminated by spray coating a solution of hexanes/PDMS, and the thicknesses of the coatings were determined following a published procedure [17]. XPS analysis was performed by BTG Labs using a Surface Science Instruments SSX-100 and a monochromatic Al K-alpha X-ray source.

2.2 Laser Processing and Surface Morphology Evaluation

Laser ablation was performed on all panels with a PhotoMachining, Inc. system with a Ekspla, Atlantic 20, frequency tripled, Nd:YVO_4 laser (6 W nominal average power at 355 nm and 200 kHz with ~10 ps pulse duration). A galvanometer was used to scan the laser spot across the stationary composite panels at a speed of 25.4 cm/s (10 in/s) during ablation. A thermopile sensor (Model 3A) and Nova II power meter from Ophir-Spiricon LLC were used to monitor the average laser power. Laser ablation produced parallel lines in the fiber direction on unidirectional CFRP laminates. Although the parameters were varied, the following is an example of a set of parameters: average power of 80 mW; pulse frequency of 400 kHz; and a line pitch of 12.7 μm (0.0005 in); which gave an overlap between two adjacent laser passes (laser spot diameter was approximately 25 μm). The scan speed was 25.4 cm/s (10 in/s) and a single-pulse fluence of 1 mJ/mm^2 and a total fluence of 24.8 mJ/mm^2. It is important to note that the single-pulse fluence is calculated with a spot size of 199.2 μm^2. The total fluence is spot size independent and accounts for energy due to overlapping pulses. Surface morphology of laser ablated CFRP (specimens coated with Pd-Au to prevent charging) was evaluated using a JEOL JSM 5600F SEM operated at an accelerating voltage of 10 to 15 kV.

2.3 Bonding and DCB Testing

Within 48 h of laser ablation, pairs of panels were bonded in an autoclave at 121 °C (250 °F) and 0.34-0.68 MPa (50-100 psi). A 7.62 cm (3 in) long, 12.5 μm thick film of FEP was included in the

layup to create a pre-crack. Using a modification of ASTM D5528-13, samples were machined with a water jet into five 2.5 cm x 24.1 cm (1 in x 9.5 in) specimens with notched ends for mounting directly on a clevis grip without need for bonding block, hinges or drilling [23]. The modified specimen geometry can be seen in Figure 1.

Prior to mechanical testing, one side of the test specimen was painted silver to improve visibility of the crack. The clevis grips were installed by opening the specimen end approximately 5 mm, and the initial crack location was marked by visual inspection with a 10× magnifying glass. An Instron® 5848 Microtester and 500 N load cell were used to record the applied load and displacement at a crosshead speed of 5 mm/min to an extension of 90 mm. A Nikon D800e camera with a 105 mm macro lens controlled with Nikon Camera Control Pro 2 software captured the crack profile once every 5 seconds up to 5 mm of crack growth and once every 15 seconds for the remainder of the test. Upon test completion, the final crack position was marked on the specimen.

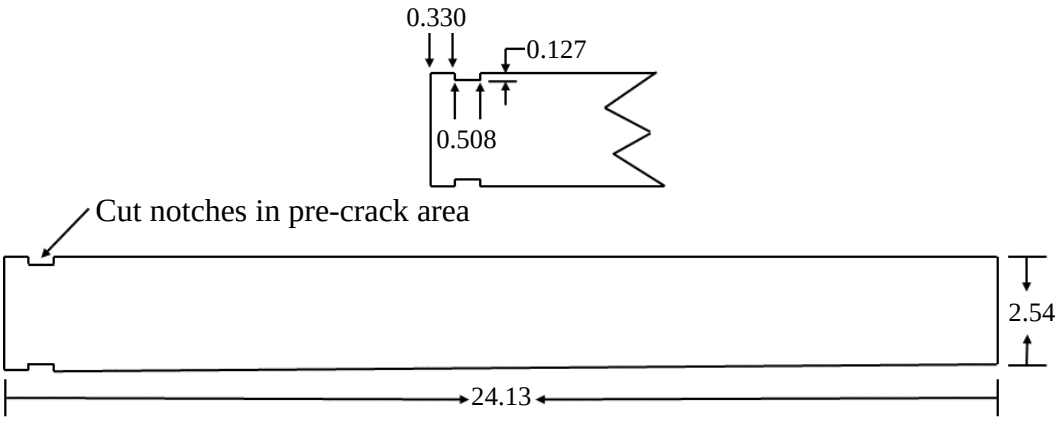

Figure 1: DCB Specimen geometry. Notches are for securing specimen to clevis grip. Measurements are in centimeters.

2.4 Failure Mode and Fracture Toughness Analysis

Failed surfaces were scanned using an Epson V600 scanner at 24 bit color and 600 dpi resolution. The failure mode was digitally analyzed by color threshold analysis using the ImageJ software, visual inspection, and guidance from ASTM D5573 [24]. Outlier values were removed for each failure mode category. The resulting data were averaged to obtain failure mode data for each test.

Crack length, load, and displacement data were used to calculate the average fracture toughness, G_{AVG}, using modified beam theory. The load vs. extension data were offset to correct for preload on the specimen caused by the modified specimen gripping technique. The G_{AVG} values were calculated for steady crack growth, which occurred primarily by cohesive failure. All crack extension data occurring prior to the maximum load point were discarded to obtain the propagation fracture toughness rather than the crack initiation value. Remaining values were assigned a weighted average based upon the percentage of crack growth they contributed, and summed to obtain G_{AVG} values for each specimen. G_{AVG} outlier values were removed for each specimen within each test.

2.5 Contact Angle Measurement

WCAs were measured using a Surface Analyst^{TM} device from BTG Labs. For all samples, WCAs were measured prior to laser ablation, immediately following laser ablation, and again prior to bonding. The post-ablation measurements were performed on identically treated areas offset from the mechanical specimen region of the panel. In this way, the area tested by WCA was not part of the bonded area in the DCB specimens and therefore could not potentially influence the test results. Nine WCA measurements were conducted on each panel for each test. The presented data are the average values from two panels.

2.6 Laser Induced Breakdown Spectroscopy

The schematic diagram of the μLIBS system is shown in Figure 2. The Nd:YVO_4 (Atlantic 20-355, EKSPLA) laser was operated at 355 nm with a nominal pulse duration of ~10 ps. The laser beam was focused by a 250 mm focal length f-theta lens (S4LFT6062/075, Sill Optics) . The LIBS emission is measured using a 328 mm, f/4.6 Schmidt-Czerny-Turner (SCT) spectrograph (IsoPlane SCT 320, Princeton Instruments). The spectral response is recorded using an electron-multiplier intensified charge-coupled device (emICCD) camera (PI-MAX4: 1024 EMB, Princeton Instruments). The plasma emission is collected with a collimator and guided to the spectrograph via an optical cable with 19 200-μm fibers. A grating with 1200 grooves/mm blazed at 300 nm and a slit width of 10 μm is used. The emICCD camera is externally triggered by the laser trigger output.

The μLIBS measurements were performed using a single laser shot on a fresh surface, and to improve the signal-to-noise ratio (SNR), 15 frames of 10 single laser shots were averaged. The 10 single laser shots were accumulated on the CCD sensor. The aim of using single-shot LIBS is to achieve a high surface sensitivity. The average laser power was measured with a thermopile sensor (3A-BB-18) and a laser power meter (Nova II, Ophir-Spiricon).

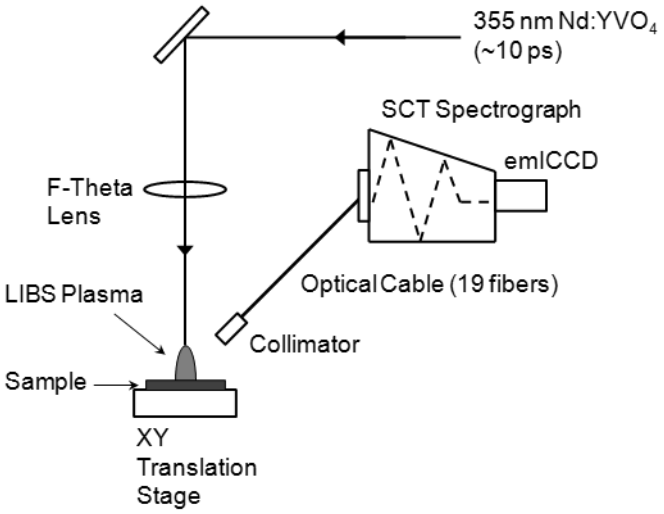

Figure 2. Schematic diagram of the μLIBS system for the detection of contaminants on CFRP.

2.7 Electron Spin Resonance Spectroscopy (ESR)

Electron paramagnetic spin resonance (ESR) spectroscopy measurements were conducted on a Varian E-line Century Series ESR Spectrometer equipped with a E102 Microwave Bridge and a V-7200 9" Magnet Assembly with a E-7600 2.5 kW Power Supply. Data acquisition and reduction were partially conducted by using the EWWin software provided by Scientific Software Services. The specimens used for ESR were from a two-ply laminate and were cut into approximately 1.5 cm × 0.3 cm in size as a proof-of-concept demonstration. The laser treatment was conducted on both top and bottom surfaces of these specimens with the laser direction parallel to the fiber direction. The specimens were fixed at the bottom of sample tubes using glass fiber so that the lateral surfaces were always parallel to the magnets (or perpendicular to the magnetic field) during measurements for consistently maximal signals. The spectra were measured at a set field of 3381 G, a modulation frequency of 100 kHz, 90° phase, a microwave frequency of 9.4 GHz, and a microwave power of 5 mW. The signal intensities reported were as-obtained first-derivative signal intensities centered at ~3450 G normalized by the specimen weight (~12 – 20 mg).

3. RESULTS & DISCUSSION

3.1 Surface Morphology

Scanning electron microscopy (SEM) micrographs of composite specimens ablated under select conditions are shown in Figure 3. Under both conditions, the ablation process selectively removed surface resin from the composite without ablating or otherwise damaging the carbon fiber.

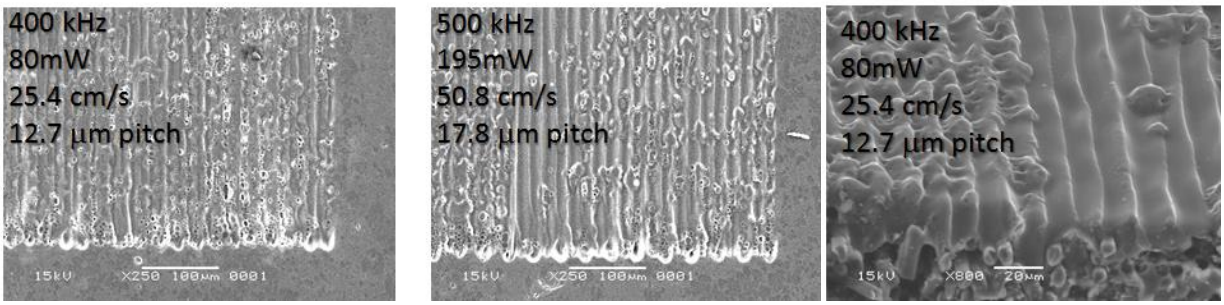

Figure 3: SEM images of ablated CFRPs surfaces under indicated conditions.

3.2 Pre-bond Surface Inspection

3.2.1 Water Contact Angle

WCA data are presented in Table 1 for the CFRP panels ablated under the laser conditions indicated in Figure 3. It is important to note that the surface topography created by the ablation process can influence the WCA results due to the feature sizes and random distribution of the roughness. The WCA measurements were conducted using a hand-held Surface Analyst^{TM} ballistic drop measurement device immediately after laser ablation and the panels were subsequently wrapped in aluminum foil and stored in a dessicator. The WCA was measured again just prior to

bonding which was within 48 hours of the laser treatment process. The data presented are an average of at least three measurements.

Table 1. WCA Measurement Results

Laser Ablation Conditions		WCA Post Ablation, °	WCA Pre-Bonding, °
#1	400kHz, 80mW, 25.4 cm/sec, 12.7 μm pitch	47.3	66.0
#2	500kHz, 195mW, 50.8 cm/sec, 17.8 μm pitch	61.4	64.1

The WCA increased significantly for both laser treatment conditions prior to bonding, but significantly more for condition 1. This suggests that the surface may have undergone some change during the time between laser treatment and bonding.

3.2.2 Laser Induced Breakdown Spectroscopy

Composite panels were contaminated with PDMS using a spray coating technique previously reported [17]. The thickness of the PDMS coatings was measured on witness silicon wafers using ellipsometry, and the coating thickness on the composite specimens was inferred from these data [17]. Coating thickness characterization is presented in Table 2.

Table 2. PDMS Coating Characterization

PDMS Thickness, nm	PDMS Areal Density, μg/cm^2
Control 0	0
17.59 ± 0.49	1.7 ± 0.05
71.53 ± 0.27	6.9 ± 0.03

An overlay of μLIBS spectra prior to laser ablation for a control CFRP sample with no PDMS, and samples with coating thicknesses of 1.7 and 6.9 μg/cm^2 are shown in Figure 4a and b for the wavelength ranges associated with carbon and silicon, respectively. The experiments were conducted with a gate delay of 10 ns (from the laser induced plasma formation), gate width of 200 ns, a pulse energy of 15 μJ and a pulse fluence of 7.53 J/cm^2. The peaks of interest are C I at 247.9 nm from carbon in the epoxy matrix resin (4a), and Si I at 288.2 nm from the PDMS contaminant (4b). It is interesting to note that the control sample, which was not intentionally contaminated with PDMS, exhibited a small peak at 288.2 nm indicating the presence of Si species, as shown in Figure 4b. XPS was conducted on the control sample, and indeed silicon (Si 2p) was detected at an atomic concentration of 4.1%. The source of silicon contamination is not known at this time.

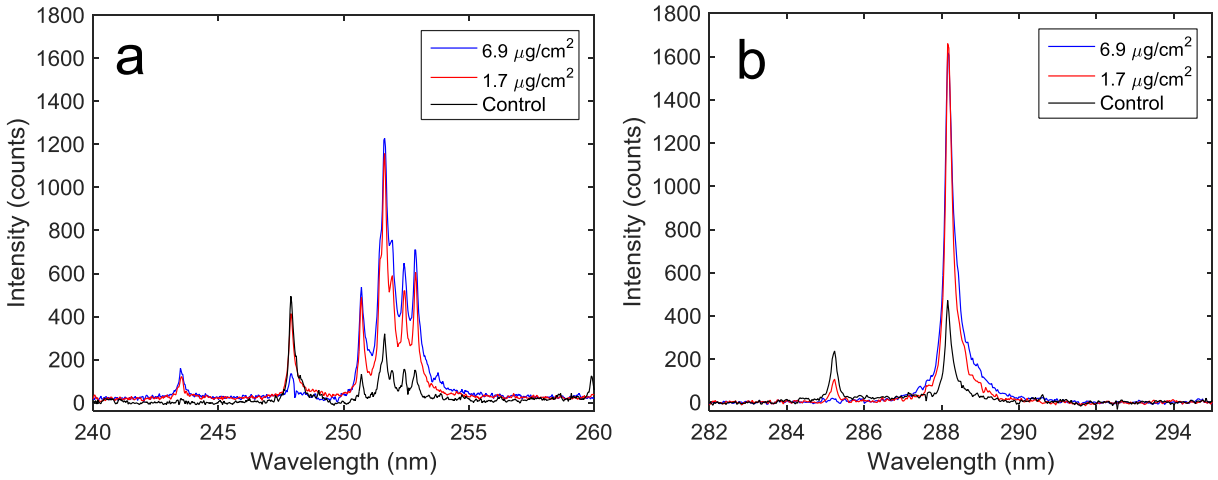

Figure 4. Overlay of μLIBS spectra prior to laser ablation, with the regions of interest for (a) C I at 247.9 nm and (b) Si I at 288.2 nm.

After characterization by μLIBS, the composite laminates were subsequently treated with the picosecond laser under the same condition as used for sample 1 in Table 1 (400kHz, 80mW, 25.4 cm/sec, 12.7 μm pitch), and then re-examined using μLIBS. The results are shown in Figure 5.

To normalize the results, the data are presented as the ratio of the Si (288.2 nm) and C (247.9 nm) peaks before (red bars) and after laser treatment (LT) (blue bars). The level of silicone contaminant was dramatically reduced after laser ablation. For the control sample, the ratio Si/C decays from 0.95 to 0.064, while for the contaminated sample with 6.9 μg/cm^2 the ratio decreases from 22.83 to 1.55. The sensitivity of the μLIBS system was able to readily detect the low level of silicone contamination (4.1 atomic % as measured by XPS) on the as-processed control laminate. Although not evident in this graph, silicone was also detected by μLIBS after laser ablation of the control specimen. Thus, μLIBS can detect silicone contaminants at concentrations significantly less than that known to pose a threat to adhesive bonding with this CFRP material system and provide real-time feedback of Si contamination levels. In addition, using the Si/C peak ratio as an analytical metric, it is possible to differentiate the control surface from the contaminated surfaces, as well as the laser treated surfaces from the untreated ones.

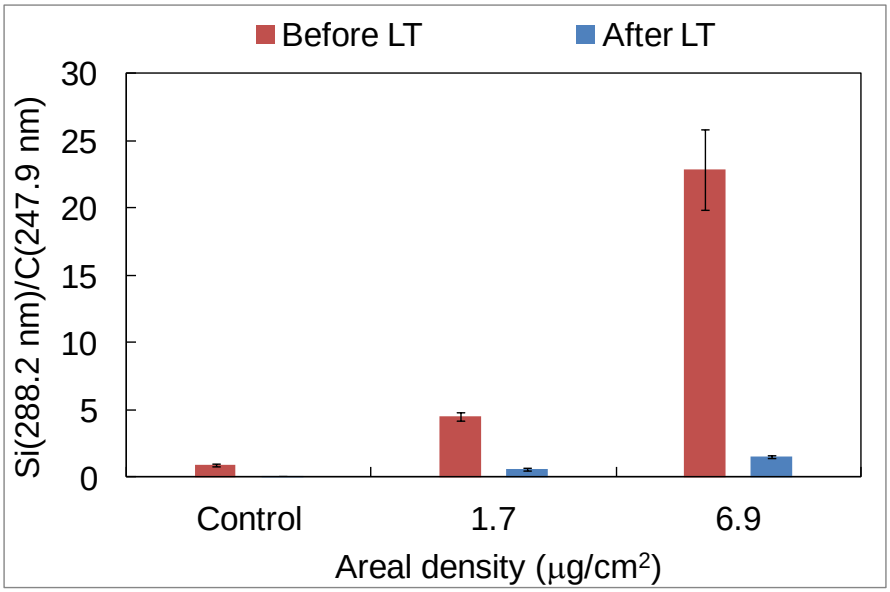

Figure 5. Ratio of the Si (288.2 nm) and C (247.9 nm) peaks before and after picosecond laser treatment (LT).

3.3 Electron Spin Resonance Spectroscopy

ESR is a technique used to measure the concentration of free-radicals, which are chemically reactive species present in the composite and can potentially react with chemical species present in the adhesive leading to covalent bond formation between the laser treated substrate and the adhesive. Experiments were conducted over a time period on a control (untreated) and laser treated composite specimens to assess the presence of free radicals (Figure 6). For the initial measurements, laser treated samples were placed in the instrument within 3 h after laser treatment. The composite samples were placed in sample tubes with a plastic cap (similar to a sample tube used in nuclear magnetic resonance spectroscopy measurements) and carefully positioned in the magnetic resonance field cavity. After measurement, the samples remained in the tubes until it was time for subsequent measurements.

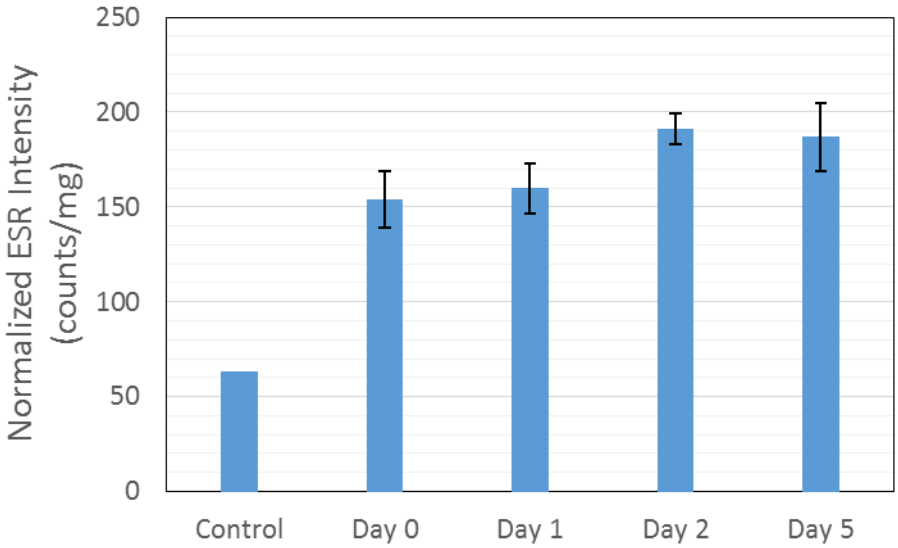

Figure 6. Normalized ESR intensity value of the specimen measured at different times after laser ablation in comparison to that of a control specimen with no laser ablation.

The ESR signal for all specimens including control and ablated samples were featured with one single line centered at ~3350 G, indicating the presence of isotropic carbon-centered free radicals with no additional coupled non-carbon nuclei [25]. Therefore, the laser treatments significantly increased their concentrations. Shown in Figure 6 are the data for a selected specimen with laser ablation conditions the same as those for condition #1 in Table 1 (400kHz, 80mW, 25.4 cm/sec, 12.7 μm pitch). The laser treatment clearly increased the concentration of free carbon radical species in the composite specimen in comparison to the control. The free radicals that formed were highly stable over the number of days measured. Separate measurements on samples under different laser treatment conditions suggested that the radicals could even be stable for a few months. More systematic evaluations regarding the dependence of free radical concentrations on different laser treatment conditions are ongoing and will be reported in the future.

3.4 Failure Mode Analysis of DCB Specimens

Failure mode analyses were conducted on DCB specimens laser treated according to both of the conditions in Table 1. Analysis of the failure mode is a critical aspect of evaluating surface treatment processes since it provides a readily apparent determination of its effectiveness. For predictable bond performance, the failure mode should be some form of cohesion. Failure modes in composites can be categorized as adherent failure (not observed for any of the specimens evaluated in this work), adhesion, and cohesion, which can be further characterized according to where within the interphase the failure occurred (see Figure 7) [23]. Failure mode analysis involves both visual inspection and image analysis to quantify the different types of failure. Images of the failed DCB specimens from laser ablation condition #1 in Table 1 are presented in Figure 7.

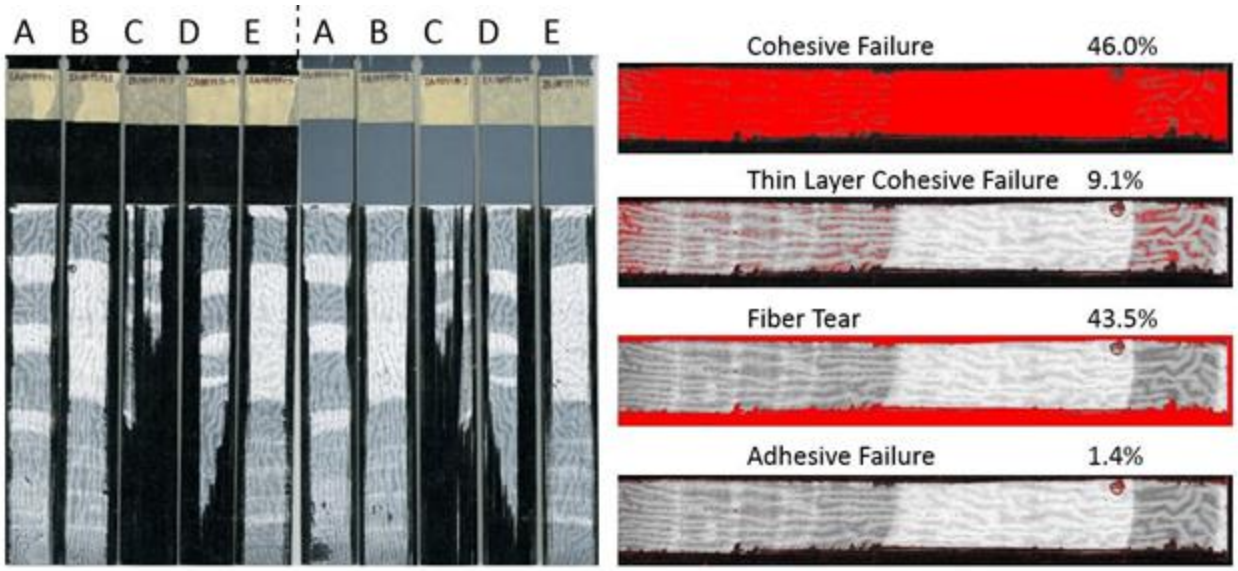

Figure 7. Scanned image (left) and ImageJ threshold analysis (right) of failed DCB specimens.

Predominantly cohesion failure was observed for the DCB specimens laser treated according to condition #1 (Table 1). A miniscule amount of adhesion failure was measured (1.4%). For the DCB specimens treated under laser ablation according to condition #2 (Table 1), a higher amount of adhesion failure was observed (11%), with the rest of the failure consisting of cohesion failure (67%), fiber tear (18.3%), and thin layer cohesive (1.8%). The results indicate that, within the error of this analysis, the laser ablation conditions are comparable with ablation condition #1 providing a slightly better surface for adhesive bonding.

3.5 Average Fracture Toughness

Fracture toughness (G_{AVG}) values are presented in Table 3 with average bondline thickness measurements. For comparison purposes, the fracture toughness obtained from this adhesive on grit blasted specimens prepared using the same composite adherends was 2.93 ± 0.12 kJ/m^2. The failure mode for these specimens was 100% cohesive.

Table 3. Average fracture toughness (G_{AVG}) and bond measurement results.

Laser Ablation Conditions	**Fracture Toughness, (kJ/m^2)**	**Bondline Thickness, (μm)**	**Adhesion Failure, %**
Control (grit blast surface treatment only)	2.93 ± 0.12	347 ± 18	0
400kHz, 80mW, 25.4 cm/sec, 12.7 μm pitch	3.03 ± 0.10	393 ± 34	1.4
500kHz, 195mW, 50.8 cm/sec, 17.8 μm pitch	2.85 ± 0.30	424 ± 28	11.0

The laser surface treated specimens exhibited a relatively small amount of adhesion failure.

4. CONCLUSIONS

A picosecond laser was used to surface treat aerospace composite laminates for adhesive bonding. The results indicated that, with the bonding system investigated, high quality adhesive bonds could be formed using this surface treatment process. A μLIBS technique was used in combination with the picosecond laser to demonstrate that minute levels of silicone contamination could be detected rapidly before and after laser ablation. In addition to spectral contaminant detection, the use of the Si/C peak ratio as an analytical parameter was used to compare the relative abundance of Si species and C from the matrix resin. The levels detected were below the amounts known to be a threat to adhesive bonding with this specific bonding system. These two methods are inherently amenable to automation and if integrated in a manner to provide closed-loop feedback control, may provide the requisite process control and analysis capability as part of an overall manufacturing methodology needed to achieve FAA certification of bonded primary airframe structures.

5. ACKNOWLEDGEMENTS

The authors thank John W. Hopkins for conducting the laser ablation surface treatment, Sean Britton and Hoa Luong for sample fabrication, and Michael Oliver for specimen preparation.

6. REFERENCES

1. Russell, J., "Advanced composite cargo aircraft proves large structure practicality," Composites World 12/04/2009, 2010.
2. Bossi, R.; Piehl, M. J., "Bonding primary aircraft structure: The issues," Manufacturing Engineering 2011, (March), 101-109.
3. Piehl, M. J.; Bossi, R. H.; Blohowiak, K. Y.; Dilligan, M. A.; Grace, W. B. "Efficient certification of bonded primary structure," SAMPE Electronic Proceedings, Long Beach, 2013; pp 649-658.
4. Kruse, T.; Fuertes, T. A. S.; Koerwien, T.; Geistbeck, M. "Bonding of CFRP primary aerospace structures - boundary conditions for certification in relation with new design and technology developments," SAMPE Electronic Proceedings, Seattle, WA, 2014.
5. Gardiner, G., "Building TRUST in bonded primary structures," Composites World, 04/01/2015.
6. Oakley, B.; Bichon, B.; Clarkson, S.; Dillingham, G.; Hanson, B.; McFarland, J. M.; Palmer, M. J.; Popelar, C.; Weatherston, M. "TRUST - A novel approach to determine effects of archetype contaminant compounds on adhesion of structural composites," SAMPE Electronic Proceedings, Baltimore, 2015.
7. Blohowiak, K. Y.; Voast, P. J. V.; Shelley, P. H.; Grob, J. W. "Nonchemical surface treatments using energetic systems for structual adhesive bonding", SAMPE Electronic Proceedings, Seattle, 2010.
8. Belcher, M. A. T.; Krieg, K. L.; Voast, P. J. V.; Blohowiak, K. Y. "Nonchemical surface treatments using atmostpheric plasma systems for structural adhesive bonding," SAMPE Electronic Proceedings, Long Beach, 2013.
9. Hart-Smith, L. J.; Redmond, G.; Davis, M. J. "The curse of the nylon peel ply," SAMPE International Symposium and Exhibition Proceedings, Vol. 41, 1-25 (1994).
10. Kanerva, M.; Saarela, O., "The peel ply surface treatment for adhesive bonding of composites: A review," International Journal of Adhesion & Adhesives, Vol. 43, 60-69 (2013).
11. Fischer, F.; Kreling, S.; Dilger, K., "Surface structuring of CFRP by using modern excimer laser sources," Physics Procedia, Vol. 39, 154-160 (2012).

12. Fischer, F.; Kreling, S.; Gaebler, F.; Delmdahl, R., "Using excimer lasers to clean CFRP prior to adhesvie bonding," Reinforced Plastics, Vol. *57*(5), 43-46 (2013).
13. Palmieri, F. L.; Watson, K. A.; Morales, G.; Williams, T.; Hicks, R.; Hicks, C. J.; Wohl, C. J.; Hopkins, J. W.; Connell, J. W. "Laser ablation surface preparation of Ti-6Al-4V for adhesive bonding," SAMPE Electronic Proceedings, Baltimore, MD, 2012.
14. Fischer, F.; Romoli, L.; Kling, R., "Laser-based repair of carbon fiber reinforced plastics," CIRP Annals - Manufacturing Technology, Vol. 59, 203-206 (2010).
15. Palmieri, F. L.; Hopkins, J.; Wohl, C. J.; Lin, Y.; Connell, J. W.; Belcher, M. A. T.; Blohowiak, K. Y. "Laser surface preparation of epoxy composites for secondary bonding: optimization of ablation depth," SAMPE Electronic Proceedings, Baltimore, MD, 2015.
16. Palmieri, F. L.; Belcher, M. A.; Wohl, C. J.; Blohowiak, K. Y.; Connell, J. W. "Laser ablation surface preparation of carbon fiber reinforced epoxy composites for adhesive bonding," SAMPE Electronic Proceedings, Long Beach, CA, 2013.
17. Palmieri, F. L.; Ledesma, R.I.; Cataldo, D.; Lin, Y.; Wohl, C. J.; Gupta, M.; and Connell, J. W. "Controlled contamination of epoxy composites with PDMS and removal by laser ablation," SAMPE Electronic Proceedings, Long Beach, CA, 2016.
18. Brune, K.; Tornow, C.; Noeske, M.; Wiesner, T.; Queiroz Barbosa, A.F.; Stamboroski, S.; Dieckhoff, S.; and Mayer, B.; "Surface analytical approaches contributing to quality assurance during manufacture of functional interfaces," Appl. Adhes. Sci., 3:2, (2015).
19. Vilmin, F.; Bazin, P.; Thibault-Starzyk, F.; Travert, A., "Speciation of adsorbates on surface of solids by infrared spectroscopy and chemometrics," Analytica Chemica Acta, Vol. 891, 79-89 (2015).
20. Oakley, B.; Bichon, B.; Clarkson, S.; Dillingham, G.; Hanson, B.; McFarland, J. M.; Palmer, M. J.; Popelar, C.; Weatherston, M., "Determination of threshold levels of archetype contaminant compounds on composite adhereds and their quantification via FTIR and contact angle techniques," Adhesion Society Proceedings, San Antonio, TX, 2016.
21. Ledesma, R.I.; Palmieri, F.L.; Yost, W.T; Connell, J.W. and Fitz-Gerald, J.M.; "Surface monitoring of CFRP structures for adhesive bonding," Adhesion Society Proceedings, St. Petersburg, FL, 2017.
22. Perey, D., "A portable surface contamination monitor based on the principle of optically stimulated electron emission (OSEE)," JANNAF Propulsion and Joint Subcommittee Meeting; 9-13, Dec. 1996; Albuquerque, NM; United States.
23. ASTM Standard D5528-13, 2013, "Standard test method for mode I interlaminar fracture toughness of unidirectional fiber-reinforced matrix composites," ASTM International, West Conshohocken, PA, 2013, www.astm.org.
24. ASTM Standard D5573-99, D5573-ADJ 1999, "standard practice for classifying failure modes in fiber-reinforced-plastic (FRP) joints," ASTM International, West Conshohocken, PA, 1999.
25. Junk, M.J.N., "Assessing the Functional Structure of Molecular Transporters by EPR Spectroscopy," Heidelberg: Springer-Verlag (2012).